Available online at www.sciencedirect.com
SCIENCE DIRECT®
Advances in Water Resources 29 (2006) 181–193
Advances in Water Resources
www.elsevier.com/locate/advwatres

Defining probability of saturation with indicator kriging on hard and soft data

Steve W. Lyon [a], Arthur J. Lembo Jr. [b], M. Todd Walter [a], Tammo S. Steenhuis [a,*]

[a] Biological and Environmental Engineering, Cornell University, Ithaca, New York 14853, USA
[b] Crop and Soil Sciences, Cornell University, Ithaca, New York 14853, USA

Received 28 February 2005; accepted 28 February 2005
Available online 19 July 2005

Abstract

In humid, well-vegetated areas, such as in the northeastern US, runoff is most commonly generated from relatively small portions of the landscape becoming completely saturated, however, little is known about the spatial and temporal behavior of these saturated regions. Indicator kriging provides a way to use traditional water table data to quantify probability of saturation to evaluate predicted spatial distributions of runoff generation risk, especially for the new generation of water quality models incorporating saturation excess runoff theory. When spatial measurements of a variable are transformed to binary indicators (i.e., 1 if above a given threshold value and 0 if below) and the resulting indicator semivariogram is modeled, indicator kriging produces the probability of the measured variable to exceed the threshold value. Indicator kriging gives quantified probability of saturation or, consistent with saturation excess runoff theory, runoff generation risk with depth to water table as the variable and the threshold set near the soil surface. The probability of saturation for a 120 m × 180 m hillslope based upon 43 measurements of depth to water table is investigated with indicator semivariograms for six storm events. The indicator semivariograms show high spatial structure in saturated regions with large antecedent rainfall conditions. The temporal structure of the data is used to generate interpolated (soft) data to supplement measured (hard) data. This improved the spatial structure of the indicator semivariograms for lower antecedent rainfall conditions. Probability of saturation was evaluated through indicator kriging incorporating soft data showing, based on this preliminary study, highly connected regions of saturation as expected for the wet season (April through May) in the Catskill Mountain region of New York State. Supplementation of hard data with soft data incorporates physical hydrology of the hillslope to capture significant patterns not available when using hard data alone for indicator kriging. With the need for water quality models incorporating appropriate runoff generation risk estimates on the rise, this manner of data will lay the groundwork for future model evaluation and development.

Keywords: Indicator kriging; Indicator semivariogram; Geostatistics; Binary logistic regression; Risk assessment

1. Introduction

To limit the pollution in waterways associated with agricultural land use (i.e., fertilizer, pesticide, and other chemicals coming from field applications), watershed managers need objective methods to identify high-risk, contaminant-contributing areas from agricultural fields. Pollution transport models are often used to rank vulnerability of contaminant sources with field-scale properties ignoring landscape position and current theories in hydrology on how and where runoff is generated [18]. Many studies demonstrate that this approach is not appropriate when considering chemical transport [9,11,17,23,42,31,38]. Quantifying probability of satura-

* Corresponding author. Tel.: +1 607 225 2489; fax: +1 607 255 4080.
E-mail addresses: sl336@cornell.edu (S.W. Lyon), ajl53@cornell.edu (A.J. Lembo), mtw5@cornell.edu (M.T. Walter), tss1@cornell.edu (T.S. Steenhuis).

0309-1708/$ - see front matter © 2005 Elsevier Ltd. All rights reserved.
doi:10.1016/j.advwatres.2005.02.012

tion to represent runoff production and nutrient transport is imperative to the development of tools based on physical hydrological mechanisms. For example, in humid, well-vegetated areas, such as in the northeastern US and many other locations, most runoff is generated by saturation excess near stream channels. Since these hydrologically active areas vary in size seasonally and during individual storm events, they are often referred to as variable source areas (VSA) [12,16]. Simulation of VSA provides the groundwork for risk-assessment tools usable by watershed planners to limit pollution that incorporate current theories in hydrology. Risk assessment tools predicting VSAs based on topographic index distributions similar to that in TOPMODEL [3] are beginning to emerge [13,45,18,34,25,26,1]. The extremely high spatial and temporal variability of soil moisture and groundwater significantly impacts many hydrological processes making development of such tools a challenge for researchers. Without methods to objectively quantify regions of runoff production, it is impossible develop risk-assessment tools incorporating the appropriate hydrological mechanisms.

As new risk-assessment tools appear, the question is raised, ''How can a high-risk region in a field be objectively quantified?'' This question requires new methods of collecting and interpreting hydrologic data to evaluate these management tools. In recent years, progress has been made in collecting snap shots of soil moisture using various remote sensing techniques [6,4,14,39,40] and field measurements [46,29,28,41,52]. These methods are powerful, but can be limited by satellite coverage, accessibility to watershed, and watershed size. Also, while spatially robust, they are often too temporally sparse (i.e., low frequency of sampling) to encompass concepts of VSAs integrated into new risk-assessment tools. High temporal resolution measurements of depth to water table are becoming readily available due to inexpensive, self-contained, water level data loggers (e.g., TruTrack, Inc). Since water table height is crucial in runoff generation, especially for saturation excess theory and during the wet season, these measurement techniques provide new information for assessing risk at the field scale. The point nature of these datasets leads naturally to geostatistical techniques to characterize spatial patterns for objective measures saturation during a rain event. With appropriate spatial interpolation techniques, temporally rich, discrete point systems generate spatial measures for hillslopes capable of capturing the dominant characteristics of VSA hydrology.

Water table elevations have been estimated through various forms of kriging and cokriging [32,10,2,7]. At the heart of any kriging methodology is the semivariogram. The semivariogram model provides a quantitative estimate of the structure required to characterize a spatial pattern from a series of point data [47]. The major structural parameters of a traditional semivariogram model include the range, sill, and nugget. The range provides a measure of the maximum distance over which spatial correlation affects the variable of interest. The sill, if it exists, represents the spatial variance of two distant measurements. The nugget represents the variance between two relatively close measurements. The nugget gives the variance in the measurement due to the inherent variability of the sampling device and the occurrence of spatial patterns smaller than the sampling interval. Within the realm of semivariogram and kriging techniques, indicator kriging provides a manner to capture extreme values [24]. Traditionally, indicator semivariograms and the resulting kriging assess risk of contamination in various constituents such as heavy metals [44,37,19] and assess uncertainty in soil properties [33,27,21]. In the most basic form, indicator semivariograms treat data as a binary indicator with respect to a threshold value (i.e., 1 if threshold is exceeded; 0 if threshold is not exceed). For a more complete discussion of indicator semivariograms and indicator kriging along with many possible derivatives in algorithms and methodology, see Goovaerts [20], Deutsch and Journel [8], and Chilès and Delfiner [5].

Western et al. [48] examined soil moisture patterns through indicator semivariograms and showed good spatial structure for high soil moisture conditions. They point out that there are shortcomings in the technique for distinguishing between connected and unconnected patterns in soil moisture. That is the semivariogram does not fully characterize the spatial structure of the pattern. Nevertheless, indicator semivariograms still have promise when applied directly to ''hard data'' or the actual measurements of the variable of interest, in the form of depth to water table for distributing runoff source areas. Areas prone to saturation either have a high ground water table or hard pan (fragipan) at shallow depth indicating landscape factors such as soil depth (i.e., available water storage capacity), upland-watershed area, and local topography as important factors determining whether or not a particular area saturate. For wet periods, interflow will be higher and often expand the extent of saturation around saturation-prone areas; conversely, dry periods will decrease interflow and extent of saturation. Thus, if the threshold value is near the soil surface, indicator semivariograms and kriging quantify the probability of saturation for an area. Another option available with indicator kriging is the incorporation of ''soft data'', or local information that is a proxy to the variable of interest and need not relate directly [20], to supplement hard data. Soft data can help compensate for a lack of spatially exhaustive observations by providing information about predictions where no hard data is available using prior probabilities [50]. With saturation excess theory and

indicator kriging incorporating soft data, regions at high-risk in terms of chemical transport and runoff production can be quantified to aide in management tool development.

This study looks at the ability of indicator semivariograms to capture probability of saturation for a hillslope in Townbrook watershed in the Catskill Mountains of New York. From this initial investigation, a manner to produce soft data to supplement the hard data observations is presented providing a method to compensate for spatially sparse data without compromising the significant hydrological features on the landscape. The spatial structure of the observations of saturated regions is improved with the incorporation of soft data. Probability of saturation maps are generated from indicator semivariograms based on the hard data, soft data, and the combination of the two. By using soft data, realistic representations of high probability of saturation regions for the rain events that capture the physical hydrology of the hillslope can be made. This gives objective quantification to measure the risk of saturation at the field scale for future model development and watershed management. As tools for evaluating nutrient management become the mode in research, this physical representation of risk assessment is needed to validate predictions of new techniques.

2. Site description and data

The 2.44 ha hillslope in this study located on New York State Department of Environmental Protection (DEP) owned lands is part of a 2 km^2 sub-watershed located in the southwest corner of the 37 km^2 Townbrook watershed in the Catskill Mountain region of New York State (Fig. 1). The hillslope ranged in elevation ranged from 585 m to 600 m above mean sea level with slopes ranged from 0° to 8°. The soils are gravelly silt loams over fractured bedrock. These shallow soils are typified as higher conductivity (5 cm/h) surface material (<40 cm deep) overlaying less conductive material (0.5 cm/h) base material (>40 cm deep) with large fractures. The landuse on the hillslope is uniformly grass/shrub with forested regions above the study area. A 200+ point survey of the region was conducted to supplement the 10 m digital elevation model (DEM) of the hillslope to derive 1-m interval contours for identifying small-scale topographic features. This supplemental elevation data was used to generate explanatory variables for the binary logistic regression analysis. Based on a multidirectional algorithm similar to that of Quinn et al. [35], upslope area was determined for the study site. Local flow paths were estimated as cells accumulating 500 m^2 of upslope area. Distance to these flow paths and the total distance to stream were evaluated along steepest surface gradient for each of the sampling locations. Topographic index, defined as $\ln[a/\tan\beta]$, and local slope at each sampling location were also evaluated.

Fig. 1 shows the layout of 43 water level loggers located on the hillslope for monitoring depth to water table. The water level loggers were WT-HR 500 capacitance probes from TruTrack, Inc. These loggers measured depth to water table in the upper 50 cm of the soil at 5-min intervals starting from March 4th, 2004 that were averaged over 15-min intervals. The loggers were placed on two grid systems. The first consisted of 19 loggers on a 10×10 m grid near the stream at the bottom of the hillslope. In addition, 24 loggers were located on a large spacing 30×40 m grid to gauge water table reactions up the hillslope. Above and below the hillslope site, two loggers were placed in the stream to function, along with a rating curve established from velocity measurements, as stream gauges. Finally, a tipping bucket rain gauge with data logger was set on the site to sample rainfall amounts at an interval of 10 min. Due to rain gauge malfunction, the rainfall data from March 23rd, 2004 to April 16th, 2004 was taken from a National Oceanic and Atmospheric Administration (NOAA) weather station located in Stamford, NY located approximately 1 km north of the hillslope. With the on-site rain gauge and NOAA station data, measures of daily rainfall amounts were created for the sampling period. From this period, six events were chosen corresponding to the largest events for the study period. Table 1 gives a summary of the six rainfall events considered in this study. These events all consisted of rainfall amounts greater than 1.5 cm on a given day and were used to investigate the formation of saturated areas on the hillslope.

3. Methods

Indicator values (I_i) were calculated by setting a threshold depth to water table (Z_c) and assigning a value of 1 to sampling locations where the measured depth to water table (z_i) was less than or equal to the threshold depth to water table and a value of 0 to locations where the depth to water table was greater than the threshold depth to water table for the rainfall event. Thus, indicator values of saturation for sampling locations during each rain event were defined as

$$I_i(z_c) = \begin{cases} 1 & \text{if } z_i \leqslant z_c \\ 0 & \text{if } z_i > z_c \end{cases} \quad (1)$$

where $I_i(z_c)$, is the indicator value at location i, z_i is the measured depth to water table at location i (in cm), and z_c is the threshold depth to water table (in cm). Sampling locations were considered in exceedence of z_c if it fit the

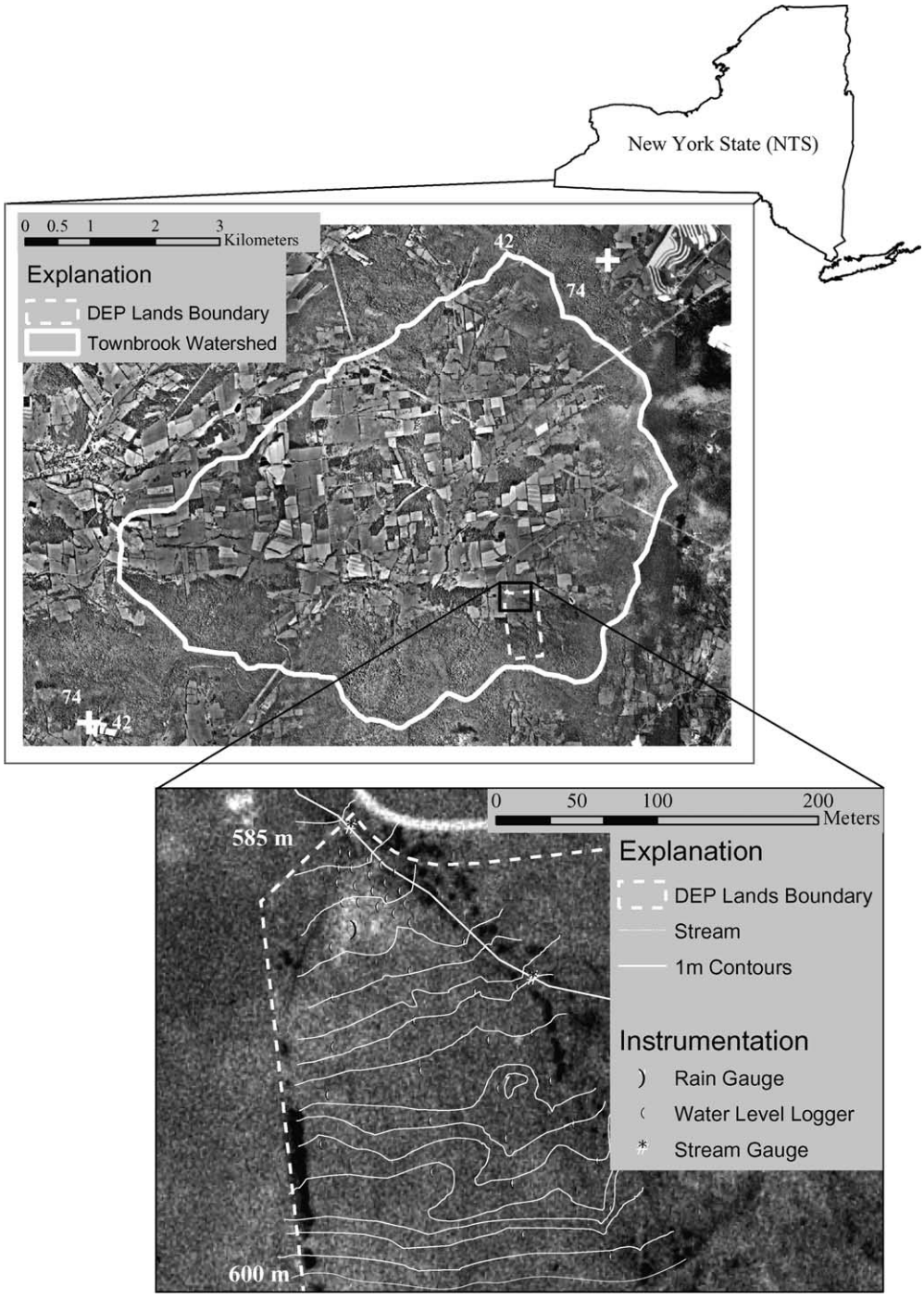

Fig. 1. Sampling locations instrumented with water level loggers on DEP lands located within Townbrook watershed in the Catskill Mountain region of New York State.

criteria of Eq. (1) for at least one 15-min interval during a rainfall event. On inspection, sampling locations that fit this criterion remained in exceedence for the majority of the rainfall event. Indicator semivariograms were constructed with GSLIB software [8] for the six rainfall events using z_c of 0 cm, 5 cm, and 10 cm based on the indicator values defined by Eq. (1) using the sample semivariance, $\gamma_s(h)$, at a lag, h, of

$$\gamma_s(h) = \frac{1}{2N(h)} \sum_{(i,j)} (I_i(z_c) - I_j(z_c))^2 \quad (2)$$

where N is the number of pairs, $I_i(z_c)$ and $I_j(z_c)$ are the indicator values at i and j, respectively, with summation over pairs (i,j) for the lag bin. This varied from standard semivariance calculations by using indicator values at points i and j instead of measured values. In order to

Table 1
Summary of six rainfall events for the study site on the DEP lands in the Townbrook watershed

Rainfall event	Date	Antecedent rainfall (10 days, mm)	Rainfall amount (mm)	Number of locations saturating		
				0 cm	5 cm	10 cm
1	4/13/2004	1.0	16.3	6	17	29
2	4/26/2004	37.9	16.5	7	22	31
3	5/2/2004	39.1	18.3	9	22	30
4	5/18/2004	18.3	17.5	4	11	21
5	5/24/2004	37.1	31.0	10	25	33
6	5/26/2004	60.5	36.1	12	28	35

make comparisons across threshold values, semivariograms were normalized with variance of the indicator values at a given threshold to create a sill value of 1 for all indicator semivariograms [8]. This method of analysis was consistent with that used by Western et al. [48] for soil moisture.

To investigate landscape factors influencing saturation, binary logistic regression was performed using MINITAB release 12 (MINITAB, Inc., 1998) to identify the most significant predictor variables of saturated regions. From the indicator semivariogram analysis, the threshold depth to water table for saturation was set 5 cm for the binary response variables. At this threshold, the semivariograms for the various rainfall events exhibit well-defined sills and ranges and there are a proportionate number of saturated and unsaturated sampling locations. Binary logistic regression procedure gives (maximum likelihood) parameter estimates that can be used to calculate the probability of saturation (π_i) at sampling location i for each event as

$$\pi_i = \log\left(\frac{1}{1-p_i}\right) = c + \beta_1 X_1 + \beta_2 X_2 + \cdots + \beta_i X_i \qquad (3)$$

where p is the probability of saturation, X_i is the set of explanatory variables, c as the intercept and β_i as the set of parameter estimates. From this, the probability of saturation was calculated from the explanatory variables as

$$p_i = \frac{\exp(\pi_i)}{1+\exp(\pi_i)} \qquad (4)$$

Binary logistic regression gave the probability of saturation based on a series of explanatory variables that were either continuous or discrete on the spatial domain. In the case of discrete variables, explanatory variables were made continuous by spatially interpolating with ordinary kriging. Thus, probability of saturation at a sampling location i was estimated using Eq. (4) with the most significant explanatory variables from Eq. (3) for each of the rainfall events. The probability model resulting from Eq. (4) provided an estimate of prior probabilities to supplement the indicator values for each location from Eq. (1) based on the significant explanatory variables found in Eq. (3) for each rainfall event. The prior probabilities are based on variables that are not direct measures of saturation, but provide a proxy to the observation of saturated areas. Thus, for each rainfall event, hard data (indicator values) and soft data (prior probabilities) were defined. These data were merged in a method consistent with Goovaerts [20] with the soft data as local indicator means respecting hard data where available. The residuals between the hard and soft data were computed at each sampling location and the semivariogram modeled.

Finally, to visualize the effects of incorporating soft data and analyze the indicator semivariograms, kriging was performed using the Geostatistical Analyst extension in ArcMap 8.2 (ESRI, Inc., 2002) with a spherical model of the form

$$\gamma_{sp}(h) = \begin{cases} \theta_s\left[\frac{3}{2}\frac{h}{\theta_r} - \frac{1}{2}\left(\frac{h}{\theta_r}\right)^3\right] & \text{for } 0 \leqslant h \leqslant \theta_r \\ \theta_s & \text{for } \theta_r < h \end{cases} \qquad (5)$$

where θ_s and θ_r as the partial sill and range parameters, respectively. The spherical model was fit by visual inspection using an interactive plotting program to avoid errors associated with blind fits by geostatistical software packages. This produced three estimates of probability of saturation derived from (1) hard data alone, (2) soft data alone, and (3) hard and soft data. The Geostatistical Analyst extension was also used to generate semivariogram surfaces for the largest and smallest rain events to investigate anisotropy in the observations on the study site.

4. Results

4.1. Indicator semivariograms—hard data

Fig. 2 shows the indicator semivariogram surfaces normalized with variance of the indicator values for saturation thresholds of 0 cm, 5 cm, and 10 cm during event 1 and event 6 to investigate anisotropy of the sampling created with the Geostatistical Analyst extension in ArcMap 8.2 (ESRI, Inc., 2002). Darker areas on the semivariogram surface correspond to larger values on the indicator semivariogram and lighter areas correspond

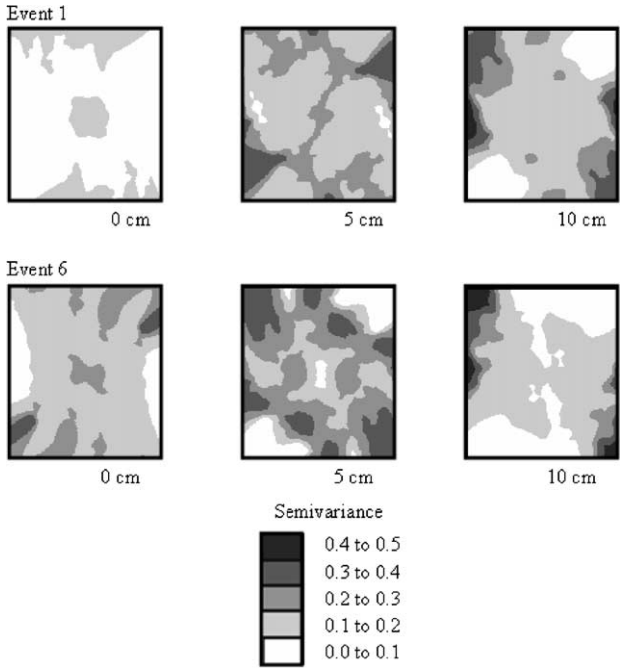

Fig. 2. Normalized indicator semivariograms surfaces for event 1 and event 6 for threshold depth to water tables of 0 cm, 5 cm, and 10 cm.

to smaller values on the indicator semivariogram. Near the center of the semivariogram surface corresponds to shorter distances on the semivariogram. Anisotropy appears as bands of dark regions occurring across the semivariogram surface showing directional trends in the semivariogram. There appears to be slight anisotropy occurring in both the northwest–southeast orientation and northeast–southwest orientation. This occurrence is not a contradiction, but corresponds to the shape of the sampling grid and topography of the hillslope (northwest–southeast orientation in the upslope and northeast–southwest orientation in the near stream region). The topography of the hillslope is too diffuse to justify incorporating anisotropy into the indictor semivariograms. In addition, the range of values of semivariance for both events is relatively low in terms of anisotropy. Thus, omnidirectional indicator semivariograms are appropriate and used for analysis of the study site.

Table 1 gives the total number of sampling locations for the six rainfall events at threshold depth to water tables of 0 cm, 5 cm, and 10 cm. These threshold depth to water tables correspond to the 19th, 49th, and 69th percentiles of observations saturating averaged over the six rainfall events. Fig. 3 shows the indicator semivariograms for the three threshold depth to water tables created with ten lag bins with a 20-meter lag distance and a tolerance of 50% so that the number of lag bins multiplied by the lag distance is half the maximum distance of the study site and the lag distance captures the sampling grid spacing. Table 2 summarizes the normalized nugget and range components of the indicator semivariograms from fitting the spherical model in Eq. (5). The indicator semivariograms exhibit pure nugget effect for all events when the threshold depth to water table is set at 0 cm attributed to spatial scarcity of the data. The sampling locations considered saturated have no spatial correlation because they are sparse and not connected on a scale capable of being captured by the sampling grid. Sampling locations are sensitive to slight undulations in the localized topography and uncertainty associated with defining the soil surface. As the threshold depth to water table is increased to 5 cm, the indicator semivariograms become smooth and exhibit better structure for events 2, 3, 5, and 6; however, events 1 and 4 still have virtually pure nugget structure. As the threshold depth to water table is raised to 10 cm, events 1 and 4 begin to show a range and structured sill. Events 2, 3, 5, and 6 begin to lose the well-defined sill and become slightly nontransitional. At a threshold depth to water table of 10 cm, the indicator semivariograms are beginning to model the water table spatial correlation and no longer capturing purely surface saturation.

The first comparison of the indicator semivariograms is the normalized nugget. This represents the ratio of measurement error to the variance of the pattern. The normalized nugget decreases for all rainfall events when the threshold depth to water table is raised from 0 cm to 5 cm. At 0 cm, few sampling locations saturate per rainfall event resulting in decreased variance for saturation (i.e., more locations are not saturated). Additional sampling locations saturate as the threshold depth to water table is raised causing the variance to increase. This result is similar to that seen by Western et al. [48] for varying thresholds of soil moistures. Also, there is a higher normalized nugget for the two lowest antecedent rainfall conditions (event 1 and event 4) at any threshold compared with the other rainfall events. This can be attributed to saturated regions smaller than the resolution captured by the sampling locations during low antecedent rainfall conditions. The next comparison of the indicator semivariograms structure is the range or the maximum distance over which pairs are considered spatially correlated. When applicable, there is an increase in range as the threshold for saturation is lowered from 5 cm to 10 cm. The indicator semivariograms begin to capture the large-scale spatial structure inherent to the water table. With threshold depth to water table at 5 cm, the indicator semivariograms are considered to capture the saturated areas that are well defined for events with high antecedent rainfall condition. For this threshold level, lower antecedent rainfall conditions do not exhibit well-defined sills and ranges. Since this threshold depth to water table captures saturated areas reasonably well without incorporating the spatial structure of the water table itself, saturation is defined as a depth to water table less than 5 cm for the remainder of this article.

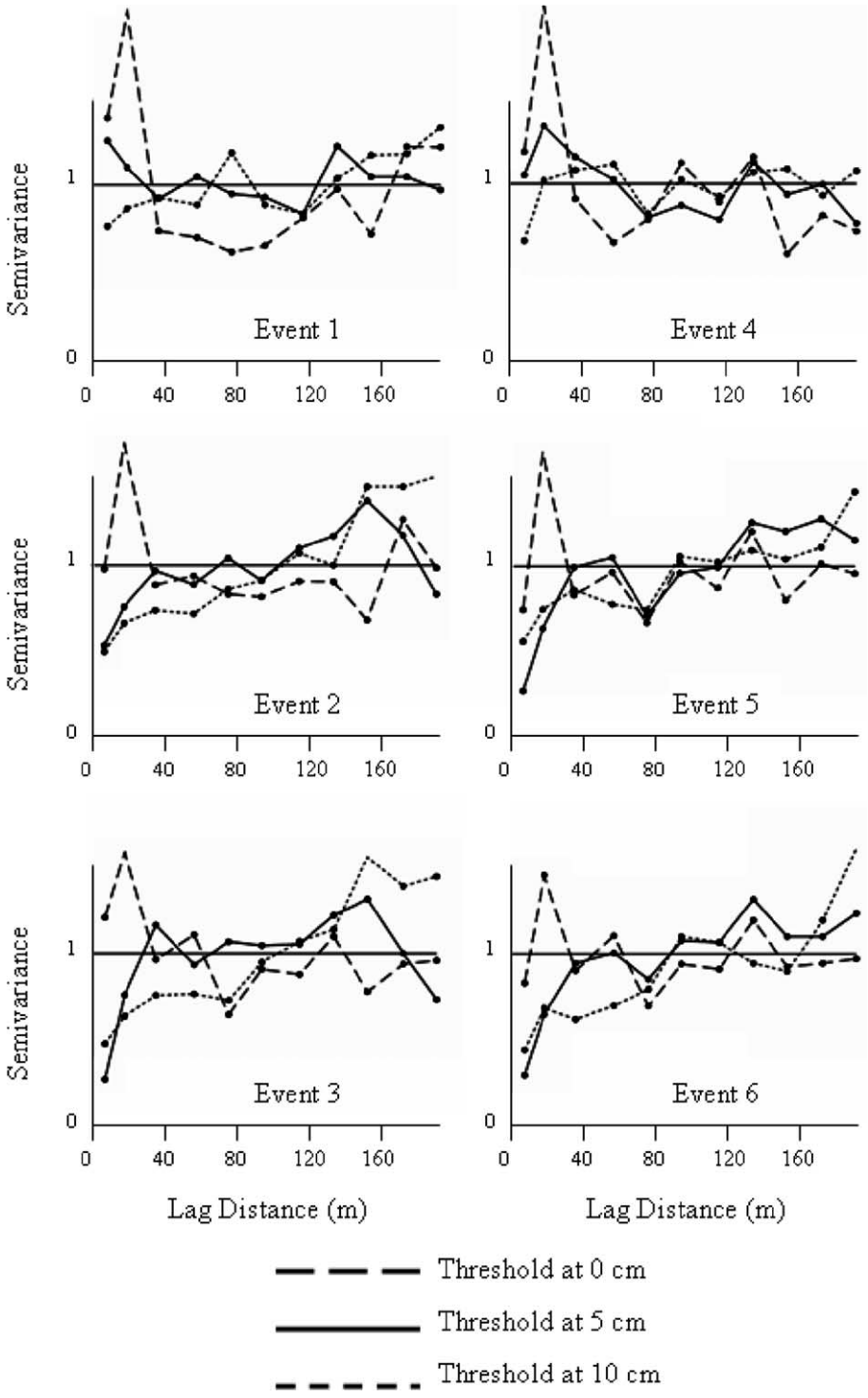

Fig. 3. Normalized indicator semivariograms for all six rainfall events with threshold depth to water tables of 0 cm (– –), 5 cm (——), and 10 cm (- - - -) using hard data alone.

4.2. Binary logistic regression—soft data

Binary logistic regression was performed to identify the significant landscape features influencing saturation. Table 3 lists and describes the explanatory variable considered for binary logistic regression analysis. Also, Table 3 gives the corresponding significance through the p-value for each explanatory variable and measures of goodness of fit for each regression with the squared Pearson's correlation coefficient, which is comparable to an R^2 for binary logistic regression. This list is by no means exhaustive, but contains explanatory variables

Table 2
Summary of normalized indicator semivariogram characteristics using hard data alone fit with spherical model with units of m for ranges

Rainfall event	Relative nugget			Range		
	0 cm	5 cm	10 cm	0 cm	5 cm	10 cm
1	1	1	0.7	0	0	60
2	1	0.35	0.4	0	65	145
3	1	0.05	0.4	0	50	150
4	1	1	0.5	0	0	30
5	1	0.1	0.45	0	75	115
6	1	0.1	0.35	0	55	170

Table 3
Explanatory variables with corresponding p-values (significant at $\alpha = 0.05$ in bold) for threshold depth to water table of 5 cm the squared Pearson's correlation coefficient in parenthesis for the binary logistic regression of each rainfall event

Explanatory variable	Variable description	p value					
		Event 1	Event 2	Event 3	Event 4	Event 5	Event 6
c	Constant	0.158	0.523	0.708	0.246	0.974	0.993
X_1	Distance from location to stream along flowpath	0.111	0.081	0.213	0.230	0.061	0.183
X_2	Distance to local flowpath accumulating more than 500 m^2	0.312	0.834	0.882	0.892	0.080	0.619
X_3	Soil type	0.172	0.519	0.620	0.857	0.944	0.852
X_4	Topographic index	0.728	0.372	0.428	0.864	0.475	0.536
X_5	Pre-event depth to water table	**0.010**	**0.020**	**0.013**	**0.018**	0.858	0.459
X_6	Total upslope area	0.481	0.832	0.499	0.664	0.338	0.520
X_7	Upslope area with maximum value truncated at 1 ha	0.405	0.680	0.728	0.818	0.520	0.834
X_8	Local slope at location	0.052	0.371	0.388	0.086	0.108	0.846

selected based on their preeminence and recurrence in hydrological theories on runoff prediction. From the binary logistic regression, the only explanatory variable that significantly estimates saturation is the pre-event depth to water table (with $\alpha = 0.05$). Event 5 and event 6 do not indicate pre-event depth to water table as a significant explanatory variable for predicting saturation. These rainfall events have the largest amounts of rainfall for all rainfall events (approximately double) with relatively high antecedent rainfall conditions. This leads to sampling locations that would typically not saturate in smaller rainfall events saturating due to the extremely large amount of the rainfall. Therefore, pre-event depth to water table is not a good predictor of saturation for these events. Using binary logistic regression, the pre-event depth to water table for the remaining four events can be used to estimate probability of saturation producing soft data to supplement hard data observations.

Soft data based on binary logistic regression was merged with the hard data observations of saturation. Ordinary kriging was used to interpolate the observations of the pre-event depth to water table for the hillslope and then probability of saturation determined from binary logistic regression. The residuals (i.e., the difference between observed saturation and probability predicted at each sampling location) were computed and modeled using a simple kriging. Fig. 4 shows the semivariograms of these residuals for events 1 through

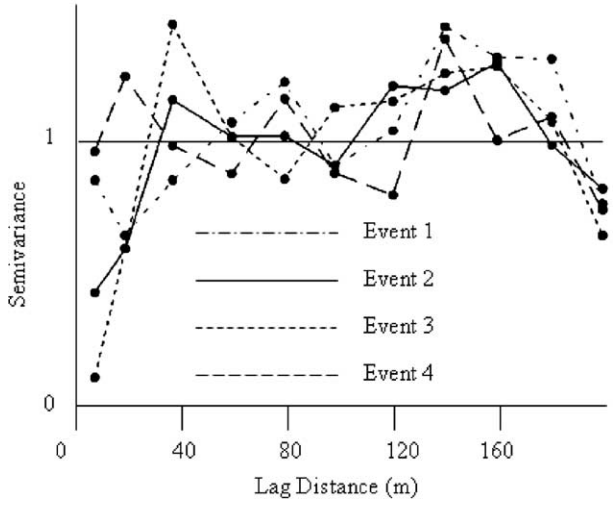

Fig. 4. Normalized residual semivariograms for threshold depth to water table of 5 cm for four rainfall events (dot-dash – event 1, solid – event 2, short dash – event 3, and long dash – event 4) between hard and soft data.

Table 4
Summary of normalized residuals semivariogram characteristics using hard and soft data fit with spherical model with units of m for ranges

Rainfall event	Normalized Nugget	Range
1	0.46	160
2	0.66	45
3	0.77	40
4	0.81	35

4. Events 5 and 6 were not modeled because they did not show pre-event depth to water table as a significant predictor of saturation. Table 4 summarizes the normalized nugget and range components of the residual semivariograms fitting the spherical model from Eq. (5). Events 2 and 3 have extremely well-defined sill and ranges of the same magnitude of the indicator semivariograms using hard data alone. The sills of the residual semivariograms for events 1 and 4 are more defined than those of the traditional indicator semivariograms. Events 1 and 4 have higher normalized nuggets than events 2 and 3. This is consistent with the traditional indicator semivariogram analysis.

4.3. Indicator kriging—hard and soft data

Fig. 5 gives the indicator kriging distributions for probability of saturation from hard data alone, soft data alone, and the hard data supplemented with the soft data indicator semivariograms for event 1 to visually demonstrate the effect of incorporating soft data on predicting saturation areas. The kriging was performed with ArcMap Geostatistical analyst that uses filters to smooth regions near actual observations producing smooth predictions maps as opposed to true indicator kriging, which would honor observations of indicator values. Fig. 5a shows the probability of saturation measurement

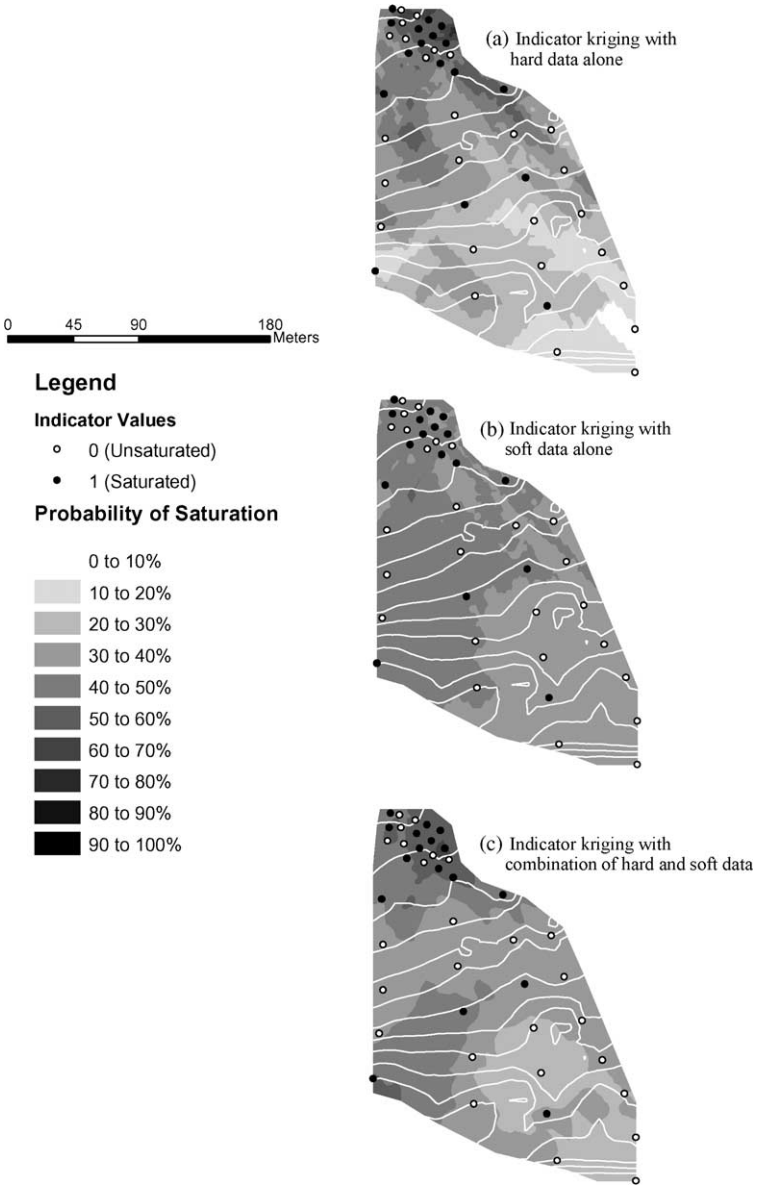

Fig. 5. Indicator kriging performed using (a) hard data alone, (b) soft data alone, and (c) hard and soft data for event 1 showing the probability of saturation for the event with indicator values marked.

Table 5
Occurrence in units of percentage of saturated and unsaturated sampling locations in estimated probability of saturations from the cross-validation analysis using all events

Estimated probability of saturation	Hard data		Soft data		Hard and soft data	
	Saturated (%)	Unsaturated (%)	Saturated (%)	Unsaturated (%)	Saturated (%)	Unsaturated (%)
0 to 25%	13	41	8	9	4	15
25 to 50%	25	41	53	52	28	49
50 to 75%	29	15	39	39	54	36
75 to 100%	33	3	0	0	14	0

from the model developed through an indictor semivariogram with hard data alone. Isolated observations of saturation located high on the hillslope produce anomalies in the prediction for high-probability saturation regions that occur in topographically divergent areas. Given that saturation excess runoff mechanisms are generally accepted to dominate in the region, it is unlikely that these high-probability saturation regions predicted with hard data alone are representative of physical hydrology of the hillslope. The kriging model developed from indictor semivariograms based on hard data alone does not define a spatial pattern using the hard data alone that is consistent with hydrological theories on how runoff is generated. The probability of saturation estimated using the soft data alone derived from the binary logistic regression analysis is shown in Fig. 5b to demonstrate predictions made through traditional binary logistic regression techniques on spatial information. Due to smoother spatial structure provided by kriging the pre-event depth to water table than in actual saturated areas, this method produces a more uniform region of high probability of saturation for the hillslope. However, by disregarding observations (i.e., the hard data) during the event, this method predicts high probability of saturation for sampling locations that do not saturate in the rainfall event. These sampling locations are positioned with little upslope area contributing to accumulation of flow. The use of soft data alone (i.e., binary logistic regression) predicts with only pre-event depth to water table and cannot capture the actual occurrence of saturation accurately due to the dynamic nature of the saturated areas during the rainfall event. Fig. 5c provides the kriging through incorporating hard and soft data. This realization provides a smoothed version of the indicator kriging using hard data alone created using the physical hydrology of the site by incorporating the structure of the pre-event depth to water table. Thus, the high probability of saturation region is more connected during this event with a low antecedent rainfall condition. Fig. 5c gives a prediction of the high-probability for saturation that agrees with the topography of the hillslope. Also, probability of saturation at locations that do not saturate during the event is better represented then through predications made from soft data alone.

This improvement is demonstrated in the cross-validation of methods presented in Table 5. Cross-validation was performed by removing one observation from the set of sample locations, performing the kriging, comparing the kriging to the left out observation, and then cycling through all the observations in all events. Table 5 shows the distribution of observations (divided into saturated or unsaturated) among the probability of saturation. Thus, 13% of saturated observations for all the events where predicted as having a probability of saturation of 0 to 25% from the cross-validation using hard data alone and only 4% of observations were in this range for the cross-validation using hard and soft data. Conversely, 3% of all unsaturated observations where predicted in the 75 to 100% probability of saturation range using hard data alone while 0% of observations were in this range for soft data alone or hard and soft data. This method of cross-validation shows that the proportion of false-positives using hard data alone is higher then when using hard and soft data combined. That is, more saturated observations are predicted as having low probability of saturation and more unsaturated observations are predicted as having high probability of saturation using the hard data alone. These false-positives are especially important when data analysis of the type is used in developing nutrient management plans or validating chemical transport models. By honoring hard data, probability of saturation is measured and not merely estimated, as it is by using soft data alone. Physically-based measures for probability of saturation are created providing an improvement over predictions made with pre-event depth to water table alone or estimates developed from observed saturation alone (i.e., soft data alone or hard data alone).

5. Discussion

By incorporating the pre-event depth to water table, we are able to supplement the hard data with soft data derived from physical hydrology of the hillslope. However, it is seen that pre-event depth to water table alone is not sufficient in prediction of saturated areas.

Since the pre-event water table is often considered as a steady state condition, this demonstrates the transient nature of saturated regions during rain events in natural systems. This result does not support the assumption linking groundwater levels and runoff as a succession

of steady-states, but is similar to the results seen in Seibert et al. [36]. Also, from the binary logistic regression analysis, it is demonstrated that traditional variables used to describe hillslope hydrology (i.e., topographic index and its constituents) may not be able to capture spatial distribution of saturated areas. Many studies have identified other controls on hydrology [22,15 49,51]. For this study, topographic features not captured in the site survey or poor resolution in subsurface characteristics may have contributed to lack of significance topographical controls in the binary logistic regression. However, the resolution of the elevation data used is much better than that for most topographically driven models where the resolution is on the order of a 10×10 m DEM. It could also indicate that new methods need to be developed for considering runoff generation, especially in shallow soil systems. New consideration of the assumptions in calculating topographic index including soil characteristics [43] or solar radiation effects [30,49] or in the topographic index's relation with groundwater [36] could be appropriate. This study demonstrates the importance in accurate prediction of pre-event ground water levels for the appropriate simulation of surface runoff.

Traditional indicator semivariograms for the six rainfall events (Fig. 3) show that there is spatial structure when there are higher antecedent rainfall conditions (events 2, 3, 5, and 6). This structure was captured with 43 sampling locations monitoring depth to water table. Due to limitations in the ability to collect high spatial resolution hydrological data for most regions, this provides a method to identify areas on the hillslope with high probability of saturation without exhaustive spatial knowledge of the entire region. From a saturation excess point of view, these regions directly correspond to regions of runoff production. During rainfall, saturated regions follow topography of the hillslope and saturate laterally from flow paths. This is similar to the results seen by Western et al. [48] for soil moisture contents during higher antecedent conditions. Thus, when high antecedent rainfall conditions (i.e., wetter initial condition) coupled with a rainfall event, saturated regions expand and are identified more readily using the water level loggers. However, due to the sparse sampling grid, it is only for rain events with high antecedent rainfall conditions when this lateral expansion is of saturated regions is large enough to be represented by the indicator semivariograms. For the smaller antecedent conditions, flow paths remain small with respect to their lateral extents and there is little spatial structure observed in saturated regions. These saturated regions are still likely to be influenced by topography and connected to the stream, but on a spatial scale smaller than that being sampled due to micro topographical features on the hillslope.

The use of high-temporal, low-spatial resolution data acquisition techniques coupled with indicator semivariogram analysis represents saturated areas in locations where other techniques are not available. Indicator approaches can incorporate soft data and this study presents one method to estimate soft data from pre-event depth to water table improving identification of high probability of saturation areas. The method takes advantage of high temporal resolution to compensate for sparse spatial coverage. As data loggers of the type used in this study become less expensive, there will be increased datasets of this variety available to the research community. These datasets are easily obtained in locations with poor satellite coverage or not accessible to mobile TDR methods of Western and Grayson [46]. By taking advantage of the data's temporal structure, fewer sampling sites are needed to obtain high quality data from a study site and provide more information about the formation of saturated areas in response to rain events of various size and intensity. We have presented only one such method to utilize the temporal resolution of the data, but others may be developed using time-series or geostatistical analysis. Results from this style of investigation lead to development of appropriate techniques to estimate pre-event depth to water table and better model saturated area formation during events. Fig. 5 gives a practical example of using geostatistics to produce a spatial distribution usable in risk assessment. Incorporation of soft data leads to a more realistic representation of the reaction of the hillslope to the rainfall event by including processes involved in the formation of saturated areas.

By actually measuring the pre-event depth to water table, factors influencing it were incorporated into the soft data without the use of proxy information (i.e., a topographic index derived from DEM). Results from this style of investigation lead to development of appropriate techniques to estimating pre-event depth to water table and better model saturated area formation during events. The use of indicator semivariograms on depth to water table leads to kriging in order to identify locations where runoff is generated. Fig. 5 gives a practical example of using geostatistics to produce a spatial distribution capable of being used in risk assessment. Incorporation of soft data leads to a more realistic representation of the reaction of the hillslope to the rainfall event. The kriging performed shows that this type of analysis also lowers the root means squared and standard error associated with the distribution. In order to correctly calibrate and validate spatial model predictions, data sets of this type are needed.

6. Conclusion

Data to quantify probability of saturation using 43 point observations and indicator kriging methods for a hillslope in the Townbrook watershed in the Catskill

Mountain region of New York State has been presented. For the six events considered, traditional indicator kriging on hard data alone captured spatial patterns in saturated regions for large antecedent rainfall conditions. However, during events with low antecedent conditions, the spatial structure provided by the indicator semivariograms were on a scale smaller than that sampled and lead to poor representations. A method to produce soft data was introduced using binary logistic regression to identify significant hydrological features that improved the spatial structure of the indicator semivariogram for lower antecedent rainfall conditions. This method to produce soft data also resulted in more realistic probability of saturation maps when kriging was conducted using the indicator semivariograms. Spatially sparse datasets supplemented with temporal data can provide better estimates of runoff source areas. As nutrient management begins to focus on timing and application of pollution sources, quantifiable identification of risk at the field scale becomes increasing important. This provides a method to collect data that, although not spatially exhaustive, still captures the physical hydrology of region in question. This type of data provides the groundwork as the next generation of nutrient transport models and risk-assessment tools develop.

Acknowledgements

Research is made possible by support and collaboration of the Department of Interior, US Geological and the Cornell University, New York Water Resources Institute under Grant Agreement No 01HQGR0208. In addition, funding of the Integrative Graduate Education and Research Traineeship (IGERT) Biogeochemistry and the Environmental Biocomplexity Program at Cornell University is acknowledged. The authors would also like to acknowledge the extremely helpful comments made by reviewers.

References

[1] Agnew LJ, Walter MT, Lembo A, Gérard-Marchant P, Steenhuis TS. Identifying hydrologically sensitive areas: bridging science and application. Hydol Process, submitted for publication.
[2] ASCE American Society of Civil Engineers Task Committee on geostatistical techniques in geohydrology. Review of geostatistics in geohydrology 1: basic concepts; 2: applications. ASCE J Hydraul Eng 1990;116(5):612–58.
[3] Beven KJ, Kirkby MJ. A physically based, variable contributing area model of basin hydrology. Hydrol Sci Bull 1979;24(1):43–69.
[4] Blyth K. The use of microwave remote sensing to improve spatial parameterization of hydrological models. J Hydro 1993;152:103–29.
[5] Chilès J-P, Delfiner P. Geostatistics: modeling spatial uncertainty. New York: Wiley; 1999.
[6] Choudhury BJ. Multispectral satellite data in the context of land surface heat balance. Rev Geophys 1991;29(2):217–36.
[7] Desbarats AJ, Logan CE, Hinton MJ, Sharpe DR. On the kriging of water table elevations using collateral information from a digital elevation model. J Hydro 2002;255:25–38.
[8] Deutsch CV, Journel AG. GSLIB: geostatistical software library and user's guide. New York: Oxford University Press; 1992.
[9] Dils RM, Heathwaite AL. Phosphorus fractionation in hillslope hydrological pathways contributing to agricultural runoff. In: Anderson MG, Brookes S, editors. Advances in hillslope processes. Chichester, UK: John Wiley & Sons Ltd; 1996.
[10] Dunlap LE, Spinazola JM. Interpolating water-table altitudes in west-central Kansas using kriging techniques. USGS water-supply paper 2238, USGS Reston, VA, 1984.
[11] Dunne T. Field studies of hillslope flow processes. In: Kirkby MJ, editor. Hillslope hydrology. New York: John Wiley & Sons; 1978.
[12] Dunne T, Black RD. Partial area contributions to storm runoff in a small New-England watershed. Water Resour Res 1970;6(5):1296–308.
[13] Endreny TA, Wood EF. Distributed watershed modeling of design storms to identify nonpoint source loading areas. J Environ Qual 1999;28(2):388–97.
[14] Engman ET. Recent advances in remote sensing in hydrology. U.S. Natl Rep Int Union Geod Geophys 1991–1994. Rev Geophys 1995;33:967–75.
[15] Famiglietti JS, Rudnicki JW, Rodell M. Variability in surface moisture content along a hillslope transect: Rattlesnake Hill, Texas. J Hydro 1998;210:259–81.
[16] Frankenberger JR, Walter MF, Boll J. Use of a GIS-based hydrological model to schedule farm manure application in the New York City watershed. Watershed restoration management: physcial, chemical, and biological considerations. New York City water supply studies. American Water Resources Association; 1996. p. 7–16.
[17] Gburek WJ, Sharpley AN. Hydrologic controls on phosphorus loss from upland agricultural watersheds. J Environ Qual 1998;27:267–77.
[18] Gburek WJ, Drungil CC, Srinivasan MS, Needelman BA, Woodward DE. Variable-source-area controls on phosphorus transport: bridging the gap between research and design. J Soil Water Conser 2002;57(6):534–43.
[19] Goovaerts P, Journel AG. Integrating soil map information in modeling the spatial variation of continuous soil properties. Eur J Soil Sci 1995;46:397–414.
[20] Goovaerts P. Geostatistics in natural resources evaluations. New York: Oxford University Press; 1997.
[21] Goovaerts P. Geostatistical modeling of uncertainty in soil science. Geoderma 2001;103:3–29.
[22] Grayson RB, Western AW, Chiew FHS, Blöschl G. Preferred states in spatial soil moisture patterns: implications for runoff and erosion control. Water Resour Res 1997;33(12):2897–908.
[23] Haygarth PM, Hepworth L, Jarvis SC. Form of phosphorus transfer and hydrological pathways from soil under grazed grasslands. Eur J Soil Sci 1998;49:65–72.
[24] Journel AG. Nonparametric estimation of spatial distributions. Math Geol 1983;15:445–68.
[25] Lindenschmidt KE, Ollesch G, Rode M. Physically-based hydrological modeling for nonpoint dissolved phosphorous transport in small and medium-sized river basins. Hydrol Sci J 2004;49(3): 495–510.
[26] Lyon SW, Walter MT, Gérard-Marchant P, Steenhuis TS. Using a topographic index to distribute variable source area runoff predicted with the SCS-curve number equation. Hydrol Proc, in press.
[27] McKenna SA. Geostatistical approach for managing uncertainty in environmental remediation of contaminated soils: case study. Environ Eng Geosci 1998;4:175–84.

[28] Meyles E, Williams A, Dowd J, Ternan L. Soil moisture patterns and runoff generation in a small Dartmoor catchment, south-west England. In: Leibundgut Ch, Uhlenbrook S, McDonnell J, editors. Runoff generation and implications for river basin modeling. Freiburger Schriften Hydrologie, band 13. Institute of Hydrology, University of Freiburg i.Br./Germany, 2001. p. 28–36.
[29] Mohanty BP, Skaggs TH, Famiglietti JS. Analysis and mapping of field-scale soil moisture variability using high-resolution, ground-based data during the Southern Great Plains 1997 (SGP97) hydrology experiment. Water Resour Res 2000;36(4): 1023–32.
[30] Moore ID, Grayson RB, Ladson AR. Digital terrain modelling: a review of hydrological, geomorphical, and biological applications. Hydrol Process 1991;5:3–30.
[31] Needleman, BA. Surface runoff hydrology and phosphorus transport along two agricultural hillslopes with contrasting soils. Ph.D. Thesis. The Pennsylvania State University, University Park, PA, 2002.
[32] Neuman SP, Jacobsen EA. Analysis of non-intrinsic spatial variability by residual kriging with application to regional groundwater levels. Math Geol 1984;16(5):499–521.
[33] Pachepsky Y, Acock B. Stochastic imaging of soil properties to assess variability and uncertainty of crop yield estimates. Geoderma 1998;85:213–29.
[34] Qiu ZY. A VSA-based strategy for placing conservation buffers in agricultural watersheds. Environ Manage 2003;32(3):299–311.
[35] Quinn P, Beven K, Chevallier P, Planchon O. The prediction of hillslope flow paths for distributed hydrological modeling using digital terrain models. Hydro Process 1991;5:59–80.
[36] Seibert J, Rodhe A, Bishop K. Simulating interactions between saturated and unsaturated storage in a conceptual runoff model. Hydro Process 2003;17:379–90.
[37] Smith JL, Halvorson JJ, Papendick RI. Using multiple-variable indicator kriging for evaluating soil quality. Soil Sci Soc Am J 1993;57:743–9.
[38] Srinivasan MS, Gburek WJ, Hamlet JM. Dynamics of storm flow generation: a field study in east-central Pennsylvania. Hydrol Process 2002;16:649–65.
[39] Troch P, Verhoest N, Gineste P, Paniconi C, Merot P. Variable source areas, soil moisture, and active microwave observations at Zwalmbeek and Coët-Dan. In: Grayson R, Blöschl G, editors. Spatial patterns in catchment hydrology: observations and modeling. Cambridge: Cambridge University Press; 2000. p. 187–208 [chapter 8].
[40] Verhoest NEC, Paniconi C, De Troch FP. Mapping basin scale variable source areas from multitemporal remotely sensed observations of soil moisture behavior. Water Resour Res 1998;24(12):3235–44.
[41] Walker JP, Willgoose GR, Kalma JD. The Nerrigundah data set: soil moisture patterns, soil characteristics, and hydrological flux measurements. Water Resour Res 2001;37(11):2653–8.
[42] Walter MT, Walter MF, Brooks ES, Steenhuis TS, Boll J, Weiler K. Hydrologically sensitive areas: variable source area hydrology implications for water quality risk assessment. J Soil Water Conser 2000;55(3):277–84.
[43] Walter MT, Steenhuis TS, Mehta VK, Thongs D, Zion M, Schneiderman E. Refined conceptualization of TOPMODEL for shallow subsurface flows. Hydrol Proc 2002;16:2041–6.
[44] Webster R, Oliver MA. Optimal interpolation and isrithmic mapping of soil properties: VI. Disjunctive kriging and mapping the conditional probability. J Soil Sci 1989;40:497–512.
[45] Weld JL, Sharpley AN, Beegle DB, Gburek WJ. Identifying critical sources of phosphorous export from agricultural watersheds. Nutr Cycl Agroecosyst 2001;59(1):29–38.
[46] Western AW, Grayson RB. The Tarrawarra data set: soil moisture patterns, soil characteristics, and hydrological flux measurements. Water Resour Res 1998;34(10):2765–8.
[47] Western AW, Blöschl G, Grayson RB. Geostatistical characterisation of soil moisture patterns in the Tarrawarra catchment. J Hydro 1998;205:20–37.
[48] Western AW, Blöschl G, Grayson RB. How well do indicator variograms capture the spatial connectivity of soil moisture? Hydrol Process 1998;12:1851–68.
[49] Western AW, Grayson RB, Blöschl G, Willgoose GR, McMahon TA. Observed spatial organization of soil moisture and its relation to terrain indices. Water Resour Res 1999;35(3):797–810.
[50] Western AW, Blöschl G, Grayson RB. Towards capturing hydrologically significant connectivity in spatial patterns. Water Resour Res 2001;37(1):83–97.
[51] Wilson DJ, Western AW, Grayson RB. Identifying and quantifying sources of variability in temporal and spatial soil moisture observations. Water Resour Res 2004;40(2):W02507.
[52] Woods RA, Grayson RB, Western AW, Duncan M, Wilson DJ, Young RI, et al. Experimental design and initial results from the Mahurangi river variability experiment: MARVEX. In: Laksnmi V, Albertson JD, Schaake J, editors. Observations and modeling of the land surface hydrological processes. Water science and application, vol. 3. AGU; 2001. p. 201–13.